Romanian Journal of Petroleum & Gas Technology
VOL. III (LXXIV) • No. 2/2022

A METHOD TO DETERMINE THE MASS FLOW TO RECIPROCATING COMPRESSORS

Paul-Octavian Dinu [1]

Ion Pană [2]

Florinel Dinu [2]

[1] SNGN ROMGAZ S.A., Natural Gas Storage Branch DEPOGAZ SRL, Ploiești, **Romania**
[2] Petroleum-Gas University of Ploiești, **Romania**
e-mail: ion.pana@upg-ploiesti.ro; flgdinu@upg-ploiesti.ro; dinup89@yahoo.com

DOI: 10.51865/JPGT.2022.02.01

ABSTRACT

To establish the mass flow to a reciprocating compressor there are several relationships used in the construction and analysis of these types of compressors. The use of relationships is based on the geometric elements of the compressor. It is also necessary to know the composition of the gas and the operating conditions with which: the adiabatic exponent, the volumetric efficiencies and the compressibility factor are determined. The paper aims to establish the compressor mass flow with the help of modern means. The modeling was done in the LMS Amesim program. We use elements from the library of program to create a virtual model of the compression system. A comparison is made with the results obtained by the classical methods. The results show that there are no big differences between the values of the mass flow obtained through the usual relations and those obtained based on the realized model, that includes the main elements necessary for a precise calculation. However, the proposed method opens a wider horizon of understanding of the compression system through direct correspondence with the real model and the graphical possibilities of displaying the time variation of the system characteristics.

Keywords: reciprocating compressors, mass flow, LMS Amesim

INTRODUCTION

Many countries are currently installing liquefied natural gas terminals, making the transition to carbon-free economies and/or adapting to current political changes. Piston compressors are energy-intensive equipment in liquefied natural gas import/export terminals. While reciprocating compressors are widely used, volumetric and energy efficiency estimation models have some shortcomings. Some process simulators, such as Aspen HYSYS or Unisim, are not properly equipped to rigorously simulate them [1]. The paper presents a procedure for the development of empirical models for predicting gas flow and mechanical work consumed, based on the process information and actual operational data. Pérez-Segarra in [2] performs a detailed analysis of the different efficiencies commonly used for the characterization of reciprocating compressors: volumetric efficiency, isentropic efficiency, mechanical efficiency and total efficiency. A procedure is presented for understanding the structure of these yields in their main components, in order to obtain a deeper perspective on the general behaviour. The developed procedure is a useful tool for comparison purposes, to characterize reciprocating compressors and to help the designers of these dynamic equipment. In [3] Roskosch introduced a model of reciprocating compressor that predicts volumetric and isentropic efficiency. In order to characterize the influence of different fluids, two semi-empirical correlations are provided for the flow rates through valves and a procedure for their use in different types of reciprocating compressors is presented. The model is validated by 63 points measured from the compressor. The calculations lead on average to prediction errors of 3.0% for isentropic yield and 2.3% for volumetric yield. One of the main factors affecting the efficiency of the reciprocating compressor is the heat transfer inside the cylinder. An analysis of heat transfer can be performed using numerical models or integral correlations. However, the accuracy of the methods is not fully verified due to the complicated experimental configuration. Tuhovcak in [4] analyses the effect of heat transfer on the efficiency of a reciprocating compressor. Various integral correlations were compared for different compressor settings and working gas compositions. The CoolProp library was used to obtain the properties of coolants and common gases. A comparison was made using the programs developed in Matlab, based on the first law of thermodynamics. The results of the theoretical analysis of the working process of the long-stroke cooling compressor with a high single-stage gas compression ratio are presented in the article [5]. The calculation method is based on the mathematical modelling of the working processes of the piston compressors. The influence of heat exchange processes through the walls of the working chamber, the processes of gas flow through the interior spaces of the compressor near the valves, the process of expansion of the free volume gas and the compressibility of the gas are taken into account. The average temperature of the injected gas was considered the efficiency criterion of the thermal working conditions. The paper [6] proposes a method for evaluating the performance in the reciprocating compressor used for natural gas. The analytical formulas of the different energies and yields for the compressor drive motor and for the reciprocating compressor are presented based on the energy balance equations. The experimental methods and parameters necessary for the calculation of energy efficiency are specified. Experimental tests on the motor compressors and separately on compressor and motor were performed under different operating conditions. According to the 4D rule for establishing the minimum allowable efficiency of the natural gas reciprocating compressors are recommended: testing of thirty-one moto compressors and twenty separate compressors selected at random. The results show that the minimum efficiency of the gas engine is 25%, of the piston compressor 85% and of the compressor motor group of 16%. The studies have been extended to the linear motors that convert the energy of high pressure gas from the pressure reducing stations at the conveyor-distributor interface. The potential energy of the high pressure gas is reduced in the natural gas pressure reducing stations when the gas passes through the reduction valves. One way to recover this energy is to use a reciprocating expansion motor coupled with an electric generator. The generator is able to produce electricity as the pressure drops by recovering potential energy. In the paper [7] was presented an advanced numerical simulation for the thermodynamic modelling of the alternative expansion engine with simple action on natural gas in different working conditions for high pressure ranges. The simulation was performed to understand the effects of different parameters and to improve engine performance. Some geometric parameters such as suction diameter, piston diameter, crank radius, connecting rod length, speed were used in this research to calculate the linear motor efficiencies.

Another use of thermodynamic process investigations inside a piston compressor cylinder, based on the volume pressure diagram, is to identify typical faults in industrial piston compressors, such as leaks through sealing rings and loosening and fluttering of the self-acting valves. The paper [8] proposes a new non-destructive method of recording the p – V diagram of the reciprocating compressor by measuring the deformation of the piston rod. An algorithm was proposed for the reconstruction of the p – V diagram based on the characteristic key points on the load curve of the piston rod. The reconstructed p – V diagrams were used to diagnose piston compressor failures being a non-destructive monitoring tool for piston compressor failures. In the paper [9], a theoretical analysis was performed to simulate natural gas piston compressors, based on the first principle of thermodynamics. To calculate the thermodynamic properties of natural gas based on the real gas model, the AGA8 state equation was used. Numerical results validated with the measured values showed a good concordance. The effects of important parameters such as: angular velocity, dead space and compression ratio on the compressor performance were studied. The results reveal that the gas temperature for the ideal gas model is higher than of the real gas model. The mass flow and mechanical work consumed for the real gas model is higher than for the ideal gas model. The article aims to determine the mass flow of a piston compressor based on a numerical model made in the LMS Amesim program. The numerical model is a virtual replica of the real model of the reciprocating compressor. The simulation includes the calculation of the volumetric and isentropic efficiencies of the compressor, during the compression and heat exchange process. This paper simplifies to some extent the approach to the issue using the component library of the LMS Amesim program. However, the construction of the model does not mean a reduction of accuracy, because the procedures based on the models recognized in different related disciplines used, with an appropriate mathematical apparatus are integrated in it. A major advantage that we emphasize is the indication of the status of the model, which shows the changes in the variables that characterize the system (33 in number) in accordance with its operation. In this way, the treated model can be better understood and correct modification decisions can be made, in order to increase the energy performance of the compression system. The screw compressors tend to replace the reciprocating compressors where possible. Interesting aspects related to the problem of their using can be found in [10-13].

THE MATHEMATICAL MODEL

As shown in the bibliographic study, some of the modern orientations are towards virtual mechanisms that reproduce the operation of real equipment and allow a better approximation of real working conditions. The model of the compression system shown in Fig. 1 contains the typical elements necessary for the operation of a compressor : the conditions (temperature and pressure) at the entrance to the compression station; conditions (temperature and pressure) at the exit of the compression station; anti-pulsating bottle at the inlet and outlet of the compressor cylinders; heat exchanger for cooling the gas between the compression stages; the two double-acting cylinders for two-stage compression; connecting pipes. The basic element of the scheme is the compressor cylinder which has a construction made in accordance with the actual equipment and a corresponding mathematical model, described below, Fig. 2. In Fig. 2 you can see the two links to the system output (1) and input (2). The cylinder model includes: valves, at which the pressure drop is set depending on the flow rate and flow area; the element enabling the characteristics of the gas to be traced; compressor cylinder; simplified model of the crank connecting rod drive system. A gas consisting entirely of methane was used. The program can use gas mixtures of up to 8 components, but the execution time increases.

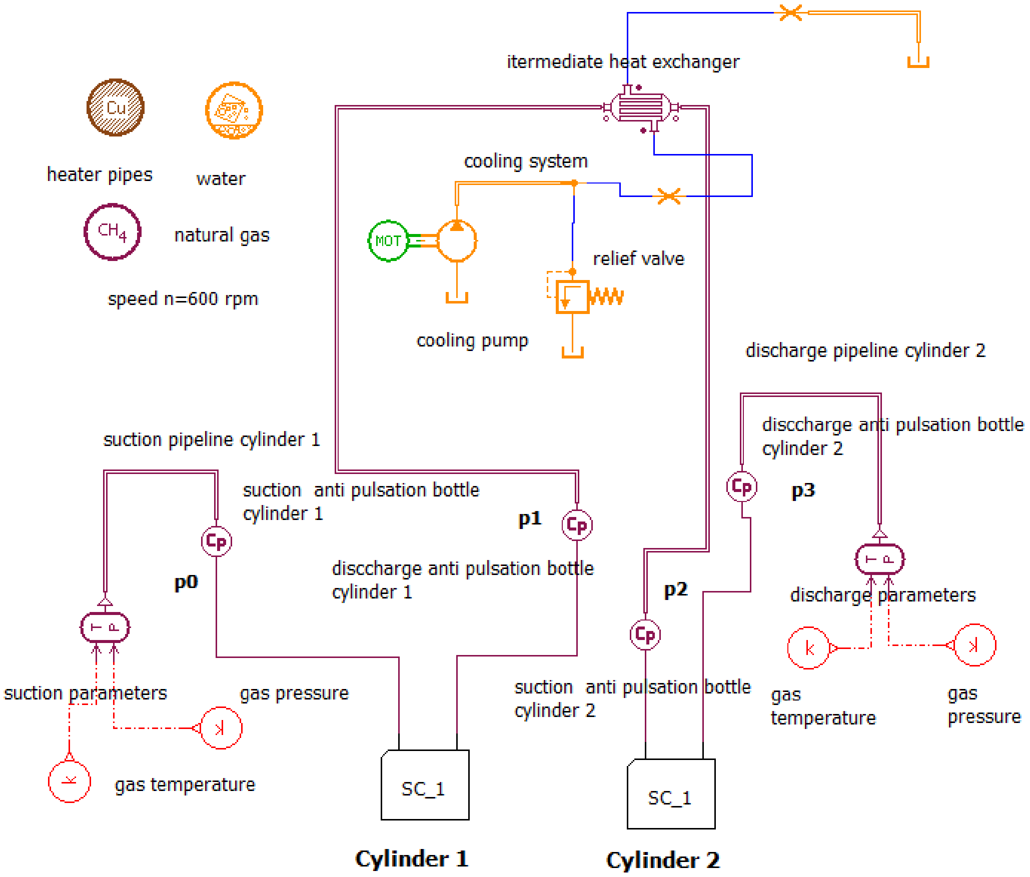

Fig. 1*. Diagram of the compression system made in the LMS Amesim program.*

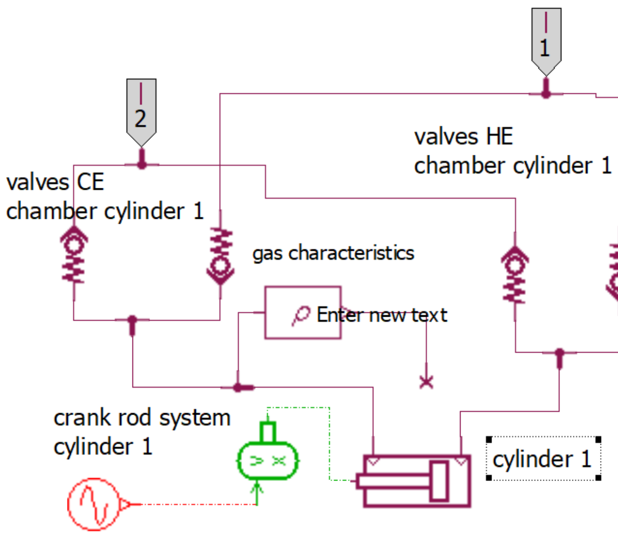

__Fig. 2.__ Diagram of the compressor cylinder in the LMS Amesim program. CE crank end, HE head end.

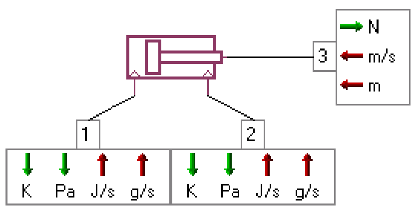

__Fig. 3.__ The main variables that characterize the pneumatic cylinder: a. at the pneumatic chambers: temperature; pressure; enthalpy; mass flow, b. at the rod: force, speed, displacement.

Regarding the model of the pneumatic cylinder it allows the introduction of geometric elements: the diameter of the piston, the stroke, the diameter of the rod, the volume of the dead space that can differ in the two chambers of the piston. Also can be introduced: the friction on the piston; the flow rate of losses along the piston; the coefficient of viscous friction in the liquid; the damping at the end of the stroke. The pneumatic cylinder as a system element includes, Fig. 3, the variables evaluated during execution, Table 1. The geometrical elements and coefficients of loss, friction, deformation are given in the Table 2. The model takes into account the initial position of the piston $xact0$. The displacement of the piston is denoted by $xact$. The pressure at the connections of the pneumatic cylinder is a gauge pressure. The calculation of the characteristics of the gas and the mass flow rate at the working pressure and temperature is made using the absolute pressure. The force is calculated using gauge pressure. The piston rod force due to viscous friction is given by the relation (1), where the A_1 is the area of the cross-section of the piston on which the p_1 pressure acts and A_2 the annular area on which the pressure acts p_2. The piston speed and the viscous friction coefficient were denoted by v and $visc$ respectively. There will be an additional force if the piston is in contact with any of the final stops. Therefore, there are three distinct modes of operation: on the lower stop if $xact \leq 0$; on the upper stop if $xact \geq stroke$, the piston stroke was denoted by *stroke;* no stops otherwise.The force at the piston rod is:

$$f_{rod} = p_1 \cdot A_1 - p_2 \cdot A_2 + v \cdot visc \qquad (1)$$

If the mode of work is on the lower stop, the next term is added to f_{rod}:

$$-k_c \cdot xact + v \cdot cdtouse1 \qquad (2)$$

where the friction coefficient $cdtouse$ is:

$$cdtouse1 = k_c \left[1 - exp\left(\frac{xact}{dist}\right)\right] \qquad (3)$$

Similarly, if on the upper stop, the next term is added to f_{rod}:

$$-k_c . (xact - stroke) + v . cdtouse2 \qquad (4)$$

where the friction coefficient $cdtouse2$ is:

$$cdtouse2 = k_c \left[1 - exp\left(\frac{xact - stroke}{dist}\right)\right] \qquad (5)$$

If there are no stops, f_{rod} is unchanged. A leakage mass flow (gas leak) can be defined as:

$$\dot{m}_{leak} = (p_1 - p_2) \cdot leak \qquad (6)$$

The corresponding flow rate of enthalpy drain (loss of enthalpy) is:

$$\dot{mh}_{leak} = \dot{m}_{leak} \cdot h \qquad (7)$$

where h is calculated using the expression:

$$h = C_{p0} \cdot \left[C_{pc} + C_{pt} \cdot \Delta T + C_{pt2} \cdot (\Delta T)^2\right] T \qquad (8)$$

where C_{p0} is the specific reference heat given at the reference temperature, C_{pc} the constant coefficient for the specific heat, C_{pt} the specific heat coefficient for the temperature term and C_{pt2} the specific heat coefficient for the squared temperature term.

The calculation of constant coefficients C_{pc}, C_{pt} , C_{pt2} can be found in [14-16]. The temperature difference is:

$$\Delta T = T_w - T_{ref} \qquad (1)$$

where T_w is the working temperature and T_{ref} is the reference temperature defined in the thermal properties of the gas. The volume of gas in the chamber corresponding to the orifice 1 is calculated as:

$$vol1 = A_1 \cdot xact + dead1 \qquad (2)$$

Similarly, for the other chamber, we have:

$$vol2 = A_2\,(stroke - xact) + dead2 \qquad (3)$$

The method of calculating the pressure and temperature variation in the pneumatic chamber is determined by the relations (16):

$$\frac{dp}{dt} = p \cdot k\left(\frac{\dot{m}}{m} - \frac{1}{V}\frac{dV}{dt}\right) \text{ (a) } \frac{dT}{dt} = \frac{k-1}{k}\frac{T}{p}\frac{dp}{dt} \text{ (b)} \qquad (4)$$

Table 1. *Variables of the pneumatic cylinder.*

No.	Variable	Notation	Unit
1	displacement of piston	xact	m
2	volume of piston chamber	vol1	cm^3
3	mass of gas in piston chamber	mgas1	g
4	volume of rod chamber	vol2	cm^3
5	mass of gas in rod chamber	mgas2	g
6	piston leakage mass flow rate	dmleak	g/s

Table 2. *Geometric elements and other elements characteristic of the pneumatic cylinder.*

No.	Variable	Notation	Unit	Value
1	initial displacement of piston	xact0	m	0
2	piston diameter	diamp	mm	508/293
3	rod diameter	diamr	mm	50.5/48.94
4	length of stroke	stroke	m	0.178
5	dead volume at port 1 end	dead1	dm^3	22/7
6	dead volume at port 2 end	dead2	dm^3	22/7
7	polytropic constant	kpoly	null	1.35
8	thermal exchange coefficient	kth	J/m^2/K/s	500
9	external temperature	extemp	K	293.15
10	viscous friction coefficient	visc	N/(m/s)	0.01
11	leakage coefficient	leak	g/s/barA	0.02
12	spring rate at endstops	k_c	N/mm	10000
13	damping coefficient on endstops	cdamp	N/(m/s)	10000
14	deformation on endstops at which damping rate is fully effective	dist	mm	0.001

Thermal calculation is based on relationships written in the matrix form (13) where m_i mass at port i (1 or 2), $h_i$enthalpy at port i (1 or 2), δQ the amount of heat exchanged.

$$\begin{bmatrix} V\cdot\left(\frac{\partial\rho}{\partial p}\right)_T & V\cdot\left(\frac{\partial\rho}{\partial T}\right)_p \\ m\cdot\left(\frac{\partial h}{\partial p}\right)_T - V & m\cdot\left(\frac{\partial h}{\partial T}\right)_p \end{bmatrix}\cdot\begin{bmatrix}\frac{dp}{dt}\\ \frac{dT}{dt}\end{bmatrix} = \begin{bmatrix} \sum\frac{dm_i}{dt} - \rho\frac{dV}{dt} \\ \sum\frac{dm_i}{dt}\cdot h_i - h\sum\frac{dm_i}{dt} + \delta Q \end{bmatrix} \quad (53)$$

The usual ratios for determining the flow to the reciprocating compressor are based on the compression ratio and the reduction of the active stroke due to the expansion of the gas in the dead space of the compressor. For a double-acting compressor the mass flow rate Q_m of the compressor is expressed by the relation:

$$Q_m = \alpha\cdot EV_a\cdot i\cdot S\cdot\frac{\pi(2D^2-d^2)}{4}\cdot\frac{P_1\cdot n}{Z_1\cdot R\cdot T_1} \quad (14)$$

where: α is the flow coefficient taking into account changes in flow direction and contraction of gas flow; this coefficient is indicated in the literature [3, 7, 10] in the domain $\alpha\in[0.7-0.95]$. The establishing of the coefficient requires a study of the conditions of entry into the compressor cylinder through the valve. In order to simplify the treatment of the proposed objective, considering that the influence of the entry conditions also appears in the classical relation (1) and in the case of the treated model and hence this coefficient was considered equal to 1; EV_a – volumetric efficiency at gas suction:

$$EV_a = 1 - m\left(\varepsilon^{1/k}-1\right) \quad (15)$$

k – adiabatic exponent of the gas mixture; ε – compression ratio:

$$\varepsilon = \frac{P_2}{P_1} \quad (16)$$

i – the number of cylinders; S – piston stroke; D – piston diameter; d – piston rod diameter; n – the number of double strokes; P – absolute pressure; p – relative pressure; Z – compressibility factor:

$$Z_1 = \frac{1}{1+\frac{527393\cdot p_1\cdot 10^{1{,}785\delta}}{T_1^{3{,}825}}} \quad (17)$$

R – constant of the gas mixture; T – absolute temperature; δ – relative density of the gas; index 1 corresponds to the conditions in the compressor stage suction; index 2 corresponds to the conditions in the compressor stage discharge. Relationship (14) has several disadvantages, but also the advantage of simplicity. The disadvantages are: in the case of multi-stage compressors we do not know the pressure at the exit of the first stage p_1; the path of the gas causing the change in pressure is not taken into account; anti-pulsating cylinders and heat exchangers are not taken into account; thermal phenomena at the cylinder level and on the pipeline path are not taken into account.

THE ANALYSIS PERFORMING AND THE RESULTS OBTAINED

As mentioned in the introductory part, the basic idea of the article is to realize a virtual model of the compression system with the help of the means available in the library of the LMS Amesim program. This way of working is evidenced by the results in Fig. 4. In the Fig. 4.a, the correlation between the pressure variation, the discharged/aspirated mass flow and the chamber volume in the external working chamber of the piston is observed. It is noticed that when increasing the pressure from 4 barA to 11 barA, the mass flow rate is null, the discharge valve of the chamber is closed. During this time from 27.00 s to 27.03 s the room volume is reduced from the maximum value of 42 l. When opening the discharge valve the gas begins to leave the working chamber, the volume of gas in the room further decreases to the value of the volume of the dead space 6 l. The discharge mass flow is variable. The pressure decreases and the gas from the dead space follows. Upon reaching the pressure of 4 barA the suction valve opens and the gas penetrates into the outer chamber, until complete filling 42 l. The suction mass flow is variable too. The suction valve closes and further the gas is compressed. During this time the parameters of the gas change, an aspect captured in Fig. 4.b for the compressibility factor, the density of the gas and the specific heat at constant pressure.

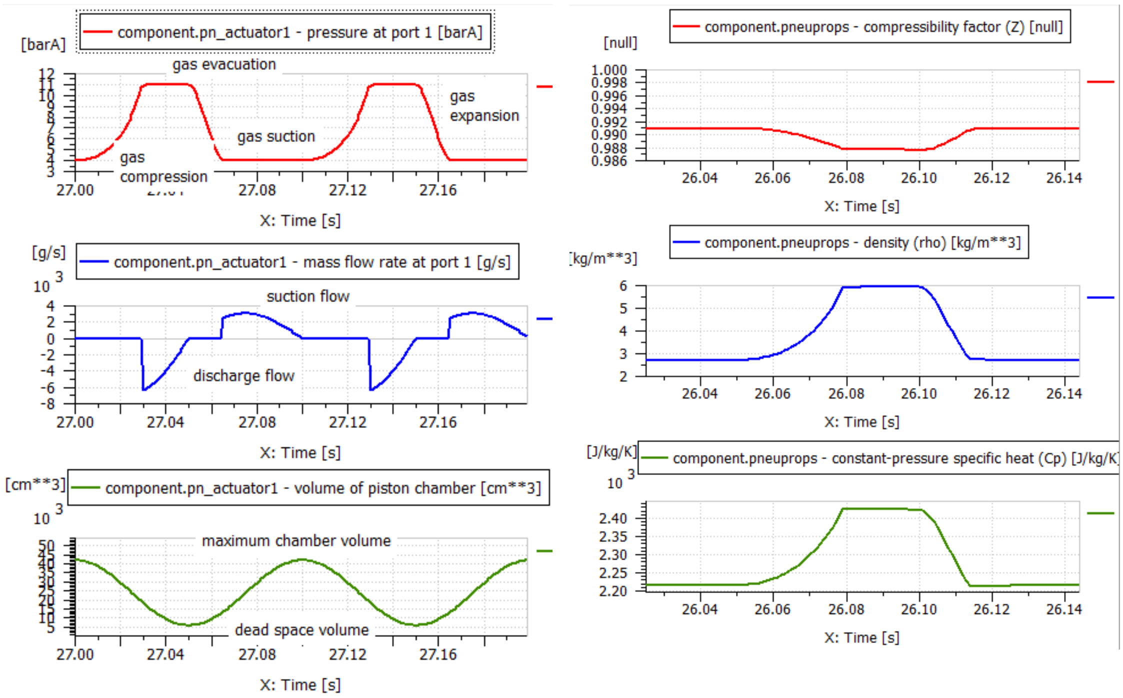

a *b*

Fig. 4*. Results of the numerical simulation for cylinder 1 of the compressor outer chamber: a. Characteristics of the compressor cylinder, from top to bottom: pressure, mass flow and chamber olume; b. variation of specific quantities for compressed gas, from top to bottom: ideal deviation factor, gas density, specific heat at constant pressure.*

The variation of these factors influences the results obtained. The model includes heat transfer to the cylinder wall, to the heat exchanger and along the pipelines. We will compare the mass of gas entering the cylinder chambers of the compressor with the gas mass appreciated on the basis of the relation (14) for a complete rotation of the crankshaft. We do this because the mass flow is variable. For the outer chamber (HE) of cylinder 1 (compression stage 1) the mass of gas deducted from the relation (1) is $\alpha \cdot EV_a \cdot S \cdot \frac{\pi \cdot D^2}{4} \cdot \frac{P_1}{Z_1 \cdot R \cdot T_1}$. The gas mass in the outer chamber (HE) of cylinder 1 can be assessed with the help of elements in the Fig. 5.

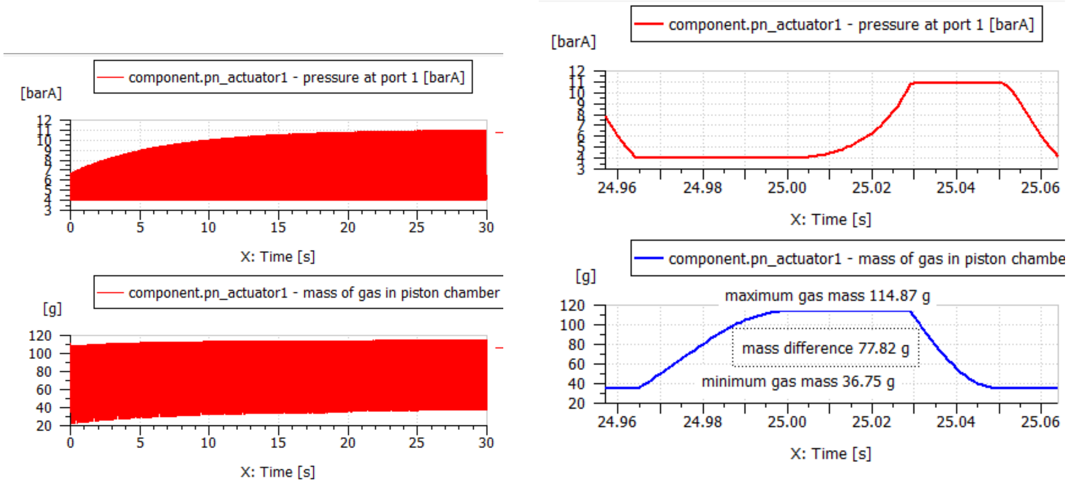

a *b*

Fig. 5. *Determination of the mass of gas entering / leaving the outer chamber of the compressor cylinder 1 at a complete rotation.*

Fig. 5.a represented the pressure (up) and the mass of gas (bottom) in the outer chamber of cylinder 1. Since the speed is 600 rpm the lines are very close and a sequence was selected during the stabilized movement Fig. 5.b. At the bottom of Fig. 5.b you can see the variation in the mass of gas in the room in accordance with the pressure variation at the top of this figure. At a complete rotation in the chamber enters / exits a gas mass of 77.82 g. It's 10 Hz frequency, so this camera has a mass flow rate of 778.2 g/s. We return with the same information for the inner chamber of cylinder 1 (stage 1) and for the two chambers of cylinder 2 (stage 2), Fig. 6a-c. Situations that have been simulated are indicated in Table 3.The cases studied are aimed at adapting the compressor to the conditions in the system are: *Case 1* suction pressure stage 1, 4 barA ; discharge pressure stage 2, 12 barA; the inlet temperature 12°C ; *Case 2* suction pressure stage 1, 3 barA; discharge pressure stage 2, 12 barA; the inlet temperature 12°C ; *Case 3* suction pressure stage 1, 2 barA; discharge pressure stage 2, 12 barA; the inlet temperature 12°C ; *Case 4* suction pressure stage 1, 3 barA; discharge pressure stage 2, 13 barA; the inlet temperature 12°C ; *Case 5* suction pressure stage 1, 3 barA; discharge pressure stage 2, 14 barA; the inlet temperature 12°C. The numerical values for the pressures in the anti-pulsating bottle at the stage 1 outlet and at the anti-pulsating bottle at the entrance to the second stage after the cooling of gas, shall be those corresponding to the numerical model made in the article. The values of the compressibility factor for the calculation of the gas masses in the second stage, used in relation (1) are calculated on the basis of the numerical model. It is noted that: the differences between the relationship of appreciation of the gas mass by the classical formula and the numerical model are very small, the deviations that occur are due to the influence of heat transfer; the numerical model allows to establish the pressures and temperatures in the anti-pulsating bottles and therefore the use of relationships (14-17); lowering the pressure at the inlet to the compressor reduces the mass flow rate; the increase in pressure at the outlet of the compressor reduces the mass flow rate.

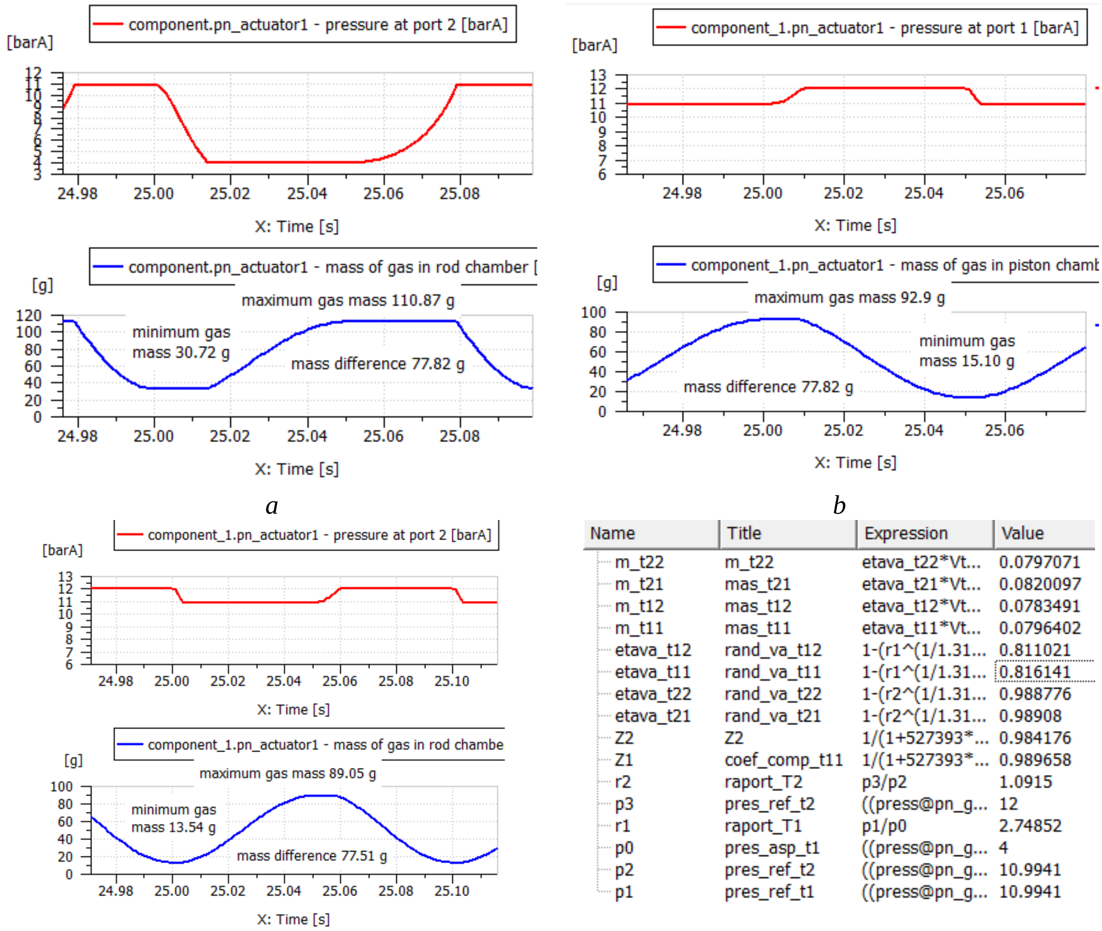

Name	Title	Expression	Value
m_t22	m_t22	etava_t22*Vt...	0.0797071
m_t21	mas_t21	etava_t21*Vt...	0.0820097
m_t12	mas_t12	etava_t12*Vt...	0.0783491
m_t11	mas_t11	etava_t11*Vt...	0.0796402
etava_t12	rand_va_t12	1-(r1^(1/1.31...	0.811021
etava_t11	rand_va_t11	1-(r1^(1/1.31...	0.816141
etava_t22	rand_va_t22	1-(r2^(1/1.31...	0.988776
etava_t21	rand_va_t21	1-(r2^(1/1.31...	0.98908
Z2	Z2	1/(1+527393*...	0.984176
Z1	coef_comp_t11	1/(1+527393*...	0.989658
r2	raport_T2	p3/p2	1.0915
p3	pres_ref_t2	((press@pn_g...	12
r1	raport_T1	p1/p0	2.74852
p0	pres_asp_t1	((press@pn_g...	4
p2	pres_ref_t2	((press@pn_g...	10.9941
p1	pres_ref_t1	((press@pn_g...	10.9941

Fig. 6. *Determination of the mass of gas entering / leaving at a complete rotation from: a. The inner chamber of cylinder 1 of the compressor; b. the outer chamber of the compressor cylinder 2; c. the inner chamber of the compressor cylinder 1 d. the values of masses and volume efficiency in the active chambers calculated on the basis of the ratios (1-4).*

Table 3*. Numerical simulation results related to the comparison between the mass flow assessment relationship (1) and the results from the numerical model of the compression system*.

Speed n = 600 rpm; The dead space factor in the head chamber of the piston is 0.158; The dead space factor in the crank piston chamber is 0.1624; Piston diameter for cylinder 1, 508 mm; Piston diameter for cylinder 2, 293 mm; Piston stroke cylinder 1 = piston stroke cylinder 2 = 177.8 mm; Cylinder 1 rod diameter, 50.8 mm; Cylinder 2rod diameter, 48.8 mm.							
1. Pressure/temperature in the anti-pulsation bottle:suction stage 1, 4 barA /13.67 °C; discharge stage 1, 10.99 barA /72.63 °C; suction stage 2, 10.97 barA / 53.56 °C; discharge stage 2, 12.0 barA / 50.26 °C.							
Gas masses in the working chambers for a complete rotation obtained on the model from LMS Amesim and based on the relation (14), HE – head end chamber, CE - crank end chamber							
Gas mass HE cylinder 1, model	**Gas mass HE, cylinder 1, rel. (1)**	**Gas mass, CE cylinder 1, model**	**Gas mass CE, cylinder 1, rel. (1)**	**Gas mass, HE cylinder 2, model**	**Gas mass HE, cylinder 2, rel. (1)**	**Gas mass, CE cylinder 2, model**	**Gas mass, CE cylinder 2, rel. (1)**
g	g	g	g	g	g	g	g
77.82	79.64	77.51	78.34	77.82	82.00	77.51	79.70
Diff.	2.31 %	Diff.	1.05 %	Diff.	5.44 %	Diff.	2.88 %
2.Pressure / temperature in the anti-pulsation bottle: suction stage 1, 3.0 barA /14.13 °C; discharge stage 1, 8.44 barA / 70.78 °C; suction stage 2, 8.42 barA / 48.36 °C; discharge stage 2, 12.0 barA / 58.14 °C.							
59.02	59.34	58.71	58.36	59.02	60.33	58.71	58.57
Diff.	0.54%	Diff.	0.59%	Diff.	1.35%	Diff.	0.23%

3. Pressure / temperature in the anti-pulsation bottle: suction stage 1, 2.0 barA /14.90 °C; discharge stage 1, 5.91 barA / 65.90 °C; suction stage 2, 5.89 barA / 40.87 °C; discharge stage 2, 12.0 barA / 64.68 °C.							
37.75	38.85	37.65	38.18	37.75	39.59	37.65	38.35
Diff.	0.25%	Diff.	0.14%	Diff.	4.8%	Diff.	1.85 %
4. Pressure / temperature in the anti-pulsation bottle; suction stage 1, 3.0 barA /14.13 °C; discharge stage 1, 8.52 barA / 71.30 °C; suction stage 2, 8.50 barA / 48.64 °C; discharge stage 2, 13.0 barA / 62.16 °C.							
58.24	59.08	57.42	58.10	58.24	60.44	57.42	58.66
Diff.	1.44%	Diff.	1.14%	Diff.	3.77%	Diff.	2.15%
5. Pressure / temperature in the anti-pulsation bottle: suction stage 1, 3.0 barA /14 °C; discharge stage 1, 8.60 barA / 71.81 °C; suction stage 2, 8.59 barA / 48.92 °C; discharge stage 2, 14.0 barA / 65.87°C.							
57.89	58.89	57.24	57.91	57.89	60.31	57.24	58.51
Diff.	1.72%	Diff.	1.17%	Diff.	7.63 %	Diff.	2.21%

CONCLUSIONS

The article is oriented towards modelling of a real system built with the help of object libraries. The model shown Fig. 1, simultaneously uses elements from several folders of the LMS Amesim library: hydraulic, pneumatic, mechanical, signal analysis. Combining them is an important element in getting closer to the real systems. This virtual model is a way of reproducing the real system with the possibility of tracking the operation and of working parameters, Fig. 4.a. The use of the Amesim LMS offers the advantage of implementing complicated and particularly accurate mathematical models for a piston compressor, Fig. 4.b. These possibilities are only partially indicated. These are numerous, for example, in Fig. 7, the mode of variation in gas pressure in the anti-pulsating bottle on the discharge of stage 1. We can establish also the temperature of the cooled gas between the steps. The heat exchanger is an element of the library, built in a way comparable to the compressor cylinder. It is possible to analyze the behavior of the compression system by tracking the influence of the changes in the system, in this case by analyzing the mass flow of the compressor. Lowering the pressure at the inlet to the compressor reduces the mass flow rate; the increase in pressure at the outlet of the compressor reduces the mass flow rate, Table 3. The classic relationships such as the expression of mass flow based on the displacement of cylinder and gas parameters at the compressor stage input, offer an accuracy comparable to modern methods. but we need the pressure at the exit of stage 1, determined with the built dynamic model.

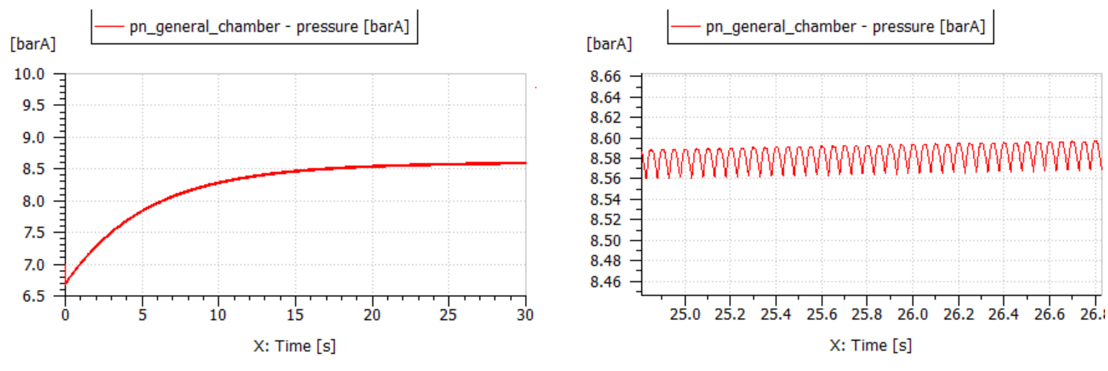

a *b*

Fig. 7. *Variation of the gas pressure in the anti-pulsating cylinder: a. variation of the pressure until the end of the transient regime; b. a detail over a short sequence of time.*

REFERENCES

[1] Harsha V.R., Vikas S.B., Harsha N.R., Arnab D., Sushant S.G., Iftekhar A.K., Shamsuzzaman F. Towards energy-efficient LNG terminals: Modeling and simulation of reciprocating compressors, Computers&Chemical Engineering,UK, vol.8, pp 312-321, 2019.

[2] Pérez-Segarra C.D., Rigola J., Sòria M., Oliva A. Detailed thermodynamic characterization of hermetic reciprocating compressors, Int. J of Refrigeration, UK, vol. 28/ issue 4, pp 579-593, 2005.

[3] Roskosch D., Venzik V., Atakan B. Thermodynamic model for reciprocating compressors with the focus on fluid dependent efficiencies, Int. J of Refrigeration, UK, vol. 84, pp 104-116, 2017.

[4] Tuhovcak J., Hejcik J., Jicha M. Comparison of heat transfer models for reciprocating compressor, Applied Thermal Engineering, vol. 103, pp 607-615, 2016.

[5] Yusha V.L., Den'gin V.G., Busarov S.S., Nedovenchanyi A.V., Gromov A.Y. The Estimation of Thermal Conditions of Highly-cooled Long-stroke Stages in Reciprocating Compressors, Procedia Engineering, Netherlands, vol. 113, pp 264-269, 2015.

[6] Zhang L., Shuangshuang L., Zheng L., Zhewei Y. Efficiency Evaluation and Experiment of Natural Gas Reciprocating Compressor. Journal of Engineering Research, Kuwait, vol. 5/ issue 2, pp 170-186, 2017.

[7] Gord M.F., Jannatabadi M. Simulation of single acting natural gas Reciprocating Expansion Engine based on ideal gas model, J of Natural Gas Science and Engineering, Netherlands, vol. 21, pp 669-679, 2014.

[8] Xueying L., Xueyuan P., Zetian Z., Xiaohan J., Zhizhong W. A new method for nondestructive fault diagnosis of reciprocating compressor by means of strain-based p–V diagram, Mechanical Systems and Signal Processing, USA, vol. 133, 2019.

[9] Farzaneh-Gord M., Niazmand A., Deymi-Dashtebayaz M., Rahbari H.R. Thermodynamic analysis of natural gas reciprocating compressors based on real and ideal gas models, Int. J of Refrigeration, UK, vol. 56, pp 186-197, 2015.

[10] Neacsu S., Eparu C.N., Neacsa A. The Optimization of Internal Processes from a Screw Compressor with Oil Injection to Increase Performances, Int. J of Heat and Technology, vol. 37/ issue 1 , pp 148-152, 2019.

[11] Eparu C.N., Neacsu S., Neacsa A., Prundurel P.A. The comparative thermodynamic analysis of compressor's energetic performance, Int. Information and Engineering Technology Association (IIETA), vol. 6/ issue 1, pp 152-155, 2019.

[12] Eparu C.N., Neacsa A., Prundurel P.A., Radulescu R., Slujitoru C., Toma N., Nitulescu M. Analysis of a high-pressure screw compressor performances, IOP Conference Series: Materials Science and Eng., vol. 595, 2019.

[13] Neacsu S., Eparu C.N., Suditu S., Neacsa A., Toma N., Slujitoru C. Theoretical and experimental features of the thermodynamic process in oil injection screw compressors, IOP Conference Series: Materials Science and Eng., vol. 595, 2019.

[14] Soave G. Equilibrium Constants from a Modified Redlich-Kwong Equation of State. Chemical Engineering Science, UK, vol. 27, pp 1197-1203, 1972.

[15] Robinson D.B., Peng D.Y. A New Two-Constant Equation of State Industrial and Engineering Chemistry: Fundamentals, Ind. & Eng. Chemistry Fundamentals, USA, vol. 15, pp 59-64, 1976.

[16] Carl L.Y. Chemical Properties Handbook, 1st Ed., McGraw-Hill Education, UK, 1999.

Received: July 2022; Accepted: July 2022; Published: August 2022